

# Towards a working density-functional theory for polymers: First-principles determination of the polyethylene crystal structure

Jesper Kleis,<sup>1</sup> Bengt I. Lundqvist,<sup>1</sup> David C. Langreth,<sup>2</sup> and Elsebeth Schröder<sup>1</sup>

<sup>1</sup>*Department of Applied Physics, Chalmers University of Technology, SE-412 96 Göteborg, Sweden*

<sup>2</sup>*Department of Physics and Astronomy, Rutgers University, Piscataway, N. J. 08854-8019*

(Dated: September 7, 2018)

Equilibrium polyethylene crystal structure, cohesive energy, and elastic constants are calculated by density-functional theory applied with a recently proposed density functional (vdW-DF) for general geometries [Phys. Rev. Lett. **92**, 246401 (2004)] and with a pseudopotential-planewave scheme. The vdW-DF with its account for the long-ranged van der Waals interactions gives not only a stabilized crystal structure but also values of the calculated lattice parameters and elastic constants in quite good agreement with experimental data, giving promise for successful application to a wider range of polymers.

PACS numbers: 31.15.Ew,36.20.Hb,71.15.Mb,61.50.Lt

Understanding of crystalline solids is greatly enhanced by the periodicity of the atomic structure, which allows very detailed comparisons between theory and experiment. Macromolecular materials, such as polymers and other complex fluids, are less well understood, due to the challenging complex natures of their structures. Features of the polymer on the atomic and mesoscopic length scales are inter-dependent. For instance, atomic bonds are on the Ångström scale, while diffusion processes involve whole chains extending some 100 Å. In order to cover the full set of length scales by theory we need atomic-scale input for mesoscopic-scale force-scheme simulations. Input forces may be determined routinely from first-principles density-functional theory (DFT) calculations, the more accurate a functional the better, for a reasonably-sized unit cell. Among polymer crystals, with their typically very complex structure, the polyethylene (PE) crystal has a relatively simple structure [1]. A first-principles implementation of DFT [2], vdW-DF, with a general account for van der Waals (vdW) forces, is here shown to give results for crystal structure, cohesive energy, and elastic constants of the PE crystal in a very promising agreement with previous low-temperature measurements.

Earlier attempts to study the equilibrium properties of polymer systems have relied on semiempirical interatomic potentials, including force-field methods [3, 4] and modified DFT calculations [5]. The fitting of internuclear potentials in order to reproduce experimental equilibrium properties gives serious restrictions on the predictive power of these methods for nonequilibrium situations and for molecules, for which experimental data are scarce or lacking. Further, these semiempirical methods lack information to make a systematic improvement of the interatomic potentials possible. A physically motivated first-principle description of sparse polymer crystals is highly desirable. When applied at perfect conditions, it might even render the possibility of developing consistent and transferable interatomic potentials for

both force schemes and hybrid methods.

The ongoing DFT success story for ground-state electron structure calculations of dense materials systems is driven by the relatively low computational cost together with the ability to describe very diverse systems. However, the widely used local and semilocal implementations do not include long-range nonlocal correlations that are essential for a proper description of the intermolecular vdW interactions. These interactions are crucial for the stability of systems with regions of low electron density, often encountered in biological and nanotechnological applications. The recently developed vdW-DF functional [2] accounts for the vdW interaction in a seamless way both at the equilibrium binding separation and at asymptotically large separations. It applies to general geometries and accounts for the nonlocal correlation via a functional that takes only the electron density as input. It has proved very promising in describing equilibrium separations and binding energies for a range of systems, including dimers of benzene rings [2, 6], graphene sheets [7], polycyclic aromatic hydrocarbons (PAH's) [8], monosubstituted benzene molecules [9], and combinations thereof, such as PAH's and phenol adsorbed on graphite [7, 10].

Simple polymer crystals constructed from long parallel polymer chains [1], such as linear PE or polypropylene, represent an important class of sparse materials that are stabilized by the vdW interaction. At low temperatures, the PE crystal stabilizes in a simple base-centered orthorhombic crystal structure (Pna<sub>2</sub>1), Fig. 1, as established by X-ray and neutron scattering experiments [11, 12, 13, 14]. Standard theory, first-principles calculations with the semilocal generalized gradient approximation (GGA) of DFT, predicts this structure to be unstable [5, 15], calling for incorporation of nonlocal interactions. Recent vdW-DF calculations on parallel, well separated PE molecules [16, 17] show the vdW interaction in these systems to be non-negligible. To account for the nonlocal correlations at all separations, in partic-

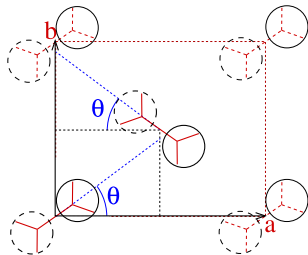


FIG. 1: Schematics of the PE crystal structure in its base-centered orthorhombic unit cell with the polymers aligned in parallel. Lattice parameters  $a$  and  $b$  are indicated, while the parameter  $c$ , which is the polymer repetition length, is perpendicular to the plane shown. Solid (broken) circles represent  $\text{CH}_2$ -units in the plane (a distance  $c/2$  out of the plane). The angular orientation of the polymers is determined by the setting angle  $\theta$ , defined as the angle between the  $a(> b)$  axis and the intra-polymer carbon plane.

ular those relevant in the PE crystal, we here apply the general-geometry vdW-DF [2].

The structure of the isolated polymer has earlier been calculated in the GGA [17], and this structure is used as input for the crystal calculations [18]. The internal geometrical structure of the isolated polymer chain thus fixes the repetition length  $c = 2.57 \text{ \AA}$  of the PE crystal unit cell.

Our vdW-DF calculations give binding-energy values at varying crystal-parameter settings, which are presented as contour maps, and from which equilibrium values for lattice parameters, cohesive energies, and elastic coefficients are extracted and compared with experimental low-temperature data. Polymers might have several conformations with similar energies. Likewise, in a polymer crystal structure several local energy minima might exist. In particular, whereas the structure shown in Fig. 1 with  $a > b$  is experimentally observed, the structure that approximately corresponds to pulling one of the polymers half a unit length ( $c/2$ ) out of the plane of the paper leads to essentially the same polymer chain packing and in turn to a similar configurational energy. In fact, the structure with a polymer pulled outward can also be described by the schematics in Fig. 1, when the requirement  $a > b$  is relaxed. Our first-principles method enables us to directly assess the cohesive-energy contours in both  $(a, b, \theta)$  regions.

The vdW-DF functional is derived and described in Ref. 2. It divides the correlation-energy functional into local and nonlocal parts,

$$E_c \approx E_c^{\text{LDA}} + E_c^{\text{nl}}, \quad (1)$$

where the first term is approximated by the local-density approximation (LDA) and the second term vanishes for a uniform system. The dispersive interactions give the sec-

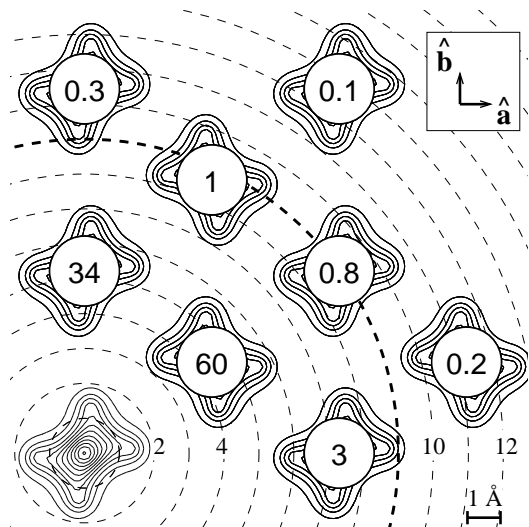


FIG. 2: The nonlocal correlation energy  $E_c^{\text{nl}}$  for pairs of PE. For the practical evaluation of  $E_c^{\text{nl}}$  in the crystal the range of integration in Eq. (2) is important. Simple pair interaction calculations give a fast estimate of the range needed, although the full calculation includes all density within the integration range. Shown here are the relative sizes (meV per polymer segment) of the polymers' contributions to  $E_c^{\text{nl}}$  (as pairs with the polymer at the circle centers), evaluated at the separations ( $\text{\AA}$ ) and relative angles shown. The contours show length-averaged electron densities. Polymers that are closer than  $9 \text{ \AA}$  (thick dashed circle) to the center polymer contribute with an energy of  $321 \text{ meV}$ . This is  $99.4\%$  of the total nonlocal correlation energy  $E_c^{\text{nl}}$  of all the polymers shown ( $323 \text{ meV}$ ).

ond term a substantial nonlocality, which allows a simpler account of the polarization properties from which it originates. It is determined from the inverse dielectric function  $\epsilon^{-1}$ , which is assumed to be dominated by a single pole, with a strength fixed by the f-sum rule. The functional form obtained approximately is

$$E_c^{\text{nl}}[n] = \frac{1}{2} \int d\mathbf{r} \int d\mathbf{r}' n(\mathbf{r}) \phi(\mathbf{r}, \mathbf{r}') n(\mathbf{r}'). \quad (2)$$

The nonlocal kernel  $\phi$  can be tabulated [2] in terms of a dimensionless distance  $D = (q_0 + q'_0)|\mathbf{r} - \mathbf{r}'|/2$  and an asymmetry parameter  $\delta = (q_0 - q'_0)/(q_0 + q'_0)$ , where  $q_0$  is a local parameter that depends on the electron density and its gradient at position  $\mathbf{r}$ . The quantity  $q_0$  is related to the pole position in  $\epsilon^{-1}$ , which is determined by the requirement that this  $\epsilon$  should give the same appropriate semilocal exchange-correlation energy density component as that of an electron gas in a much better approximation.

The nonlocal-energy integral (2) has the electronic density  $n(\mathbf{r})$  as input. We use a self-consistently determined GGA density with the revPBE exchange flavor [2, 19, 20], calculated for the full crystal unit cell using a plane-wave code [21] with ultrasoft pseudopotentials [22]. The plane-wave basis set is truncated at  $400 \text{ eV}$ , and a  $(4 \times 4 \times 10)$   $k$ -point Monkhorst-Pack sampling of the Brillouin zone

is used for the the periodically repeated unit cell. A spatial sampling separation of 0.13 Å between fast-Fourier-transform grid points is used.

In Ref. 2 the vdW-DF is described for and applied to finite molecules. The generalization to extended systems is straightforward. For an adsorbate system (a finite molecule plus an extended surface) this is described in Ref. 7. For a bulk system, like the PE crystal,  $E_c^{\text{nl}}[n]$  of the crystal unit cell must include the interactions from the surrounding cells. This is taken care of by letting the spatial integrals in Eq. (2) (as energy per unit cell) extend over the unit cell for  $\mathbf{r}$  and “everywhere” for  $\mathbf{r}'$ . In practice, the  $\mathbf{r}'$  integral is carried out over a region in space that is sufficiently large, i.e. by adding more space we do not change  $E_c^{\text{nl}}$  at the desired level of accuracy. We find it sufficient to include a total of 5 unit cells in each of the  $a$  and  $b$  directions (Fig. 1) and 9 unit cells in the  $c$  direction in the  $\mathbf{r}'$  integral, by which  $E_c^{\text{nl}}$  is found to deviate less than one part per thousand from the results obtained by integrating over a substantially larger region of space. Figure 2 illustrates this by showing the pairwise contributions to the polymer interaction  $E_c^{\text{nl}}$ . The figure shows that the most important contributions come from the nearest and next-nearest neighbor polymers.

The total energy of the crystal is thus

$$E_{\text{vdW-DF}} = E_{\text{GGA}} - E_{\text{GGA},c} + E_{\text{LDA},c} + E_c^{\text{nl}}, \quad (3)$$

with the revPBE flavor of GGA. The cohesive energy is obtained as the difference between the calculated total-energy values for the actual structure and for a reference structure with widely separated PE polymers. The electron-density-grid spacing as well as the polymer position relative to the grid are kept fixed for the vdW-DF reference calculation to ensure that any polymer self-interaction of the crystal calculation and most grid-related numerical errors are canceled by the reference calculation. The scheme applies also to other sparse-matter systems.

The cohesive-energy contours of the PE-crystal, that is the loci of equal binding-energy values for configurations with varying values of the lattice parameters  $a$ ,  $b$  and the setting angle  $\theta$  (Fig. 3), are calculated with vdW-DF, and two nearly equally deep minima are found at two different setting-angle values (Table I). The configuration approximately sketched in Fig. 1 is the most stable of the two. However, the two configurations are very close in energy, differing by only 1 meV/CH<sub>2</sub> (1%), and an accuracy sufficiently high to resolve such a stability issue cannot be claimed for the vdW-DF method.

The calculated values of equilibrium lattice parameters for the Fig. 1 structure are in close agreement with the experimental ones (Table I), the vdW-DF values ( $a_0, b_0$ ) = (7.30 Å, 5.22 Å) differing by at most 8% from the experimentally observed values. The calculated values of the cohesive energy (not including zero-point fluc-

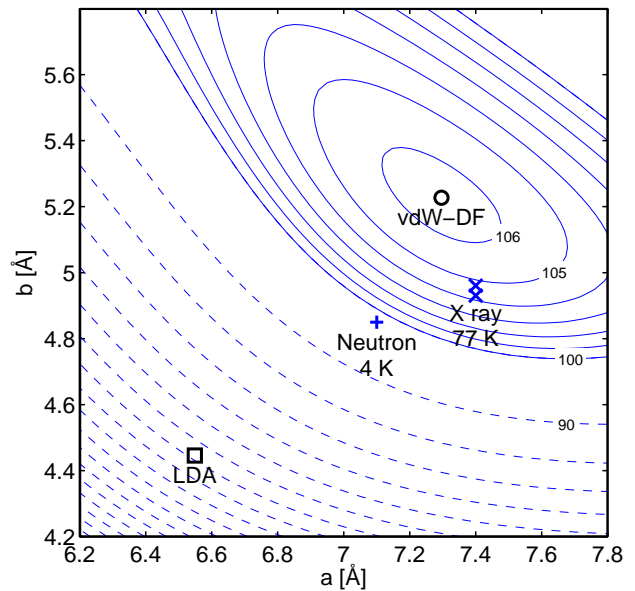


FIG. 3: The cohesive-energy contour map calculated with vdW-DF, expressed as energy per CH<sub>2</sub> group as a function of the lattice parameters  $a$  and  $b$ . The plot (but not the calculation) is restricted to show the energetics at setting angle  $\theta = 44^\circ$ , which is the optimal angle found with vdW-DF (Table I). The unit-cell height is fixed to  $c = 2.57$  Å. The full (dashed) contour curves are separated by 1 (10) meV/CH<sub>2</sub>, with values given in meV/CH<sub>2</sub> at selected contours. The equilibrium parameters (summarized in Table I) obtained from experiments and from a LDA-DFT study are shown for comparison.

tuations) and the elastic coefficients (Table I) are also in good accord with experiments.

In comparison with other attempts to calculate the PE-crystal equilibrium data (Table I), the vdW-DF results show a very promising agreement with experimental data. This is, indeed, in great contrast to the fact that the PE-crystal is unstable in GGA, according to earlier studies [5, 15, 23] and confirmed here, and also to the clear overbinding of the LDA [23]. Calculations with ad-hoc corrections for the dispersive interactions [27] with the BLYP functional [5] and with the force-field method [3] give results in a fair agreement with experimental data. However, the former uses an empirically damped  $-R^{-6}$  internuclear potential [5], and the latter has parameters fitted to experimental data at 4 K, such as lattice parameters [3], providing agreement with experiment at this temperature by construction. As a contrast, the vdW-DF calculations do not take any empirical input.

The vdW-DF functional used here combines the correlation-energy functional  $E_c^{\text{nl}}$  (Eq. (2)) with an exchange functional taken from the revPBE flavor of GGA. Although the latter closely represents the Hartree-Fock exchange at separations relevant for this work, it gives

TABLE I: Values of equilibrium lattice parameters  $a_0$  and  $b_0$ , setting angle  $\theta_0$ , elastic constants  $C_{11}$ ,  $C_{12}$ , and  $C_{22}$ , and cohesive energy  $E_{\text{coh}}$  per  $\text{CH}_2$  group, calculated by the vdW-DF method and compared with other theoretical and experimental data.

Method	$C_{11}$ (GPa)	$C_{12}$ (GPa)	$C_{22}$ (GPa)	$E_{\text{coh}}$ (eV/ $\text{CH}_2$ )	$a_0$ (Å)	$b_0$ (Å)	$\theta_0$ (degr.)
vdW-DF	11.1	6.3	8.9	0.106 <sup>j</sup>	7.30	5.22	44
vdW-DF	8.8	6.7	12.8	0.105 <sup>j</sup>	5.29	7.28	51
LDA <sup>a</sup>	41.2	11.3	47.1	0.11 <sup>j</sup>	6.55	4.45	44.4
LDA+BLYP+6-LJ <sup>b</sup>	14.1	7.2	11.8	0.11 <sup>j</sup>	7.40	4.90	45
Force field (4 K) <sup>c</sup>	14.0	7.9	13.5	0.081	7.20	4.80	41.9
Neutrons (77K) <sup>d</sup>	11.5						
Experiment <sup>e</sup>				0.080			
X rays (77 K) <sup>f</sup>					7.42	4.96	47.7
X rays (77 K) <sup>g</sup>					7.39	4.93	45
Neutrons (4 K) <sup>h</sup>					7.12	4.85	41
Experiment (213 K) <sup>i</sup>	8.4	4.2					

<sup>a</sup>Ref. 23. <sup>b</sup>Ref. 5. <sup>c</sup>Ref. 3. <sup>d</sup>Ref. 24. <sup>e</sup>Ref. 25. <sup>f</sup>Ref. 12. <sup>g</sup>Ref. 13. <sup>h</sup>Ref. 14. <sup>i</sup>Ref. 26.

<sup>j</sup>Value not corrected for zero-point motion, estimated to account for approximately 0.01 eV/ $\text{CH}_2$ .

a slight misrepresentation of the true exchange repulsion [2, 6, 9]. An analysis of the PE-molecule density profile implies that this effect should be stronger in the  $b$  than in the  $a$  direction, which is indeed the case for our calculated results. Thus an improved exchange description should give an even better agreement with the experimental geometry.

In summary, the vdW-DF method successfully predicts structural, cohesive, and elasticity data for the important test case of the PE crystal. It is gratifying that the inclusion of the fully nonlocal vdW-DF correlation functional [Eq. (2)], which has no empirical input or fitted parameters, leads to a good agreement with experimental data. As similar conclusions are drawn for a variety of different carbon-based systems, like graphene, dimers of benzene, polyaromatic hydrocarbons, monosubstituted benzene molecules, and combinations thereof [6, 7, 8, 9, 10], the vdW-DF functional is certainly very promising for general kinds of geometries and molecules, like those in macromolecular materials.

Support from the Swedish Research Council and the Swedish National Graduate School in Materials Science, as well as allocation of computer resources at UNICC (Chalmers) and SNIC (Swedish National Infrastructure for Computing), is gratefully acknowledged. Work by D.C.L. was supported in part by NSF Grant DMR-0456937.

[1] D.L. Dorset, Rep. Prog. Phys. **66**, 305 (2003).

[2] M. Dion et al., Phys. Rev. Lett. **92**, 246401 (2004); **95**, 109902(E) (2005).

[3] N. Karasawa, S. Dasgupta, and W.A. Goddard III, J. Phys. Chem. **91**, 2263 (1991).

[4] R. A. Sorensen et al., Macromol. **21**, 200 (1988).

[5] S. Serra et al., Chem. Phys. Lett. **331**, 339 (2000).

[6] A. Puzder, M. Dion, and D.C. Langreth, J. Chem. Phys. **124**, 164105 (2006).

[7] S.D. Chakarova-Käck et al., Phys. Rev. Lett. **96**, 146107 (2006).

[8] S.D. Chakarova-Käck, J. Kleis, and E. Schröder, *Dimers of polycyclic aromatic hydrocarbons in density functional theory*, Applied Physics Report 2005-16.

[9] T. Thonhauser, A. Puzder, and D.C. Langreth, J. Chem. Phys. **124**, 164106 (2006).

[10] S.D. Chakarova-Käck et al., Phys. Rev. B. **74**, 155402 (2006).

[11] C.W. Bunn, Trans. Faraday Soc. **35**, 482 (1939).

[12] P.W. Teare, Acta Cryst. **12**, 294 (1959).

[13] S. Kavesh and J.M. Schultz, J. Polym. Sci. A-2 **8**, 243 (1970).

[14] G. Avitabile et al., J. Polym. Sci., Polym. Lett. Ed. **13**, 351 (1975).

[15] B. Montanari and R. O. Jones, Chem. Phys. Lett. **272**, 347 (1997).

[16] J. Kleis, P. Hyldgaard, and E. Schröder, Comp. Mat. Sci. **33**, 192 (2005).

[17] J. Kleis and E. Schröder, J. Chem. Phys. **122**, 164902 (2005).

[18] We find that for separations typical in the PE crystal, the influence on the internal geometry from neighboring polymer chains is negligible.

[19] Y. Zhang and W. Yang, Phys. Rev. Lett. **80**, 890 (1998).

[20] D.C. Langreth et al., Int. J. Quantum Chem. **101**, 599 (2005).

[21] DACAPO from <http://wiki.fysik.dtu.dk/dacapo>

[22] D. Vanderbilt, Phys. Rev. B **41**, 7892 (1990).

[23] M.S. Miao et al., J. Chem. Phys. **115**, 11317 (2001).

[24] J.F. Twistleton, J.W. White, and P.A. Reynolds, Polymer **23**, 578 (1982).

[25] F.W. Billmeyer, J. Appl. Phys. **28**, 1114 (1957).

[26] C.L. Choy and W.P. Leung, J. Polym. Sci., Polym. Phys. Ed. **23**, 1759 (1985).

[27] See Refs. 5–11 in Ref. 7.